

# EFFECT OF ASPECT RATIO ON TORSIONAL CAPACITY OF HIGH-STRENGTH PLAIN CONCRETE DEEP BEAMS

Tamim A. Samman and Talal A. Radain  
Assistant Professors of Structural Engineering  
King Abdulaziz University, Jeddah, Saudi Arabia.

## ABSTRACT

Twenty high-strength plain concrete deep beams were tested under torsion. The variables were concrete strength and depth/width (aspect) ratio. Concrete strengths of 51.01, 58.53, 76.60 and 83.66 MPa and depth/width (aspect) ratios varying from 1 to 5 were used. The tested beams failed suddenly and violently along a smooth surface. The crack inclinations on the beam surfaces were influenced by the concrete strength and aspect ratio. Test results show that by increasing the concrete strength or by reducing the aspect ratio, the torsional capacity and the beam stiffness increases while the angle of twist decreases. A modification has been suggested to the strength equation of the ACI Code 318-89 for normal-strength concrete shallow beams under torsion to include the effect of high-strength concrete for deep beams. The proposed equation gave a good estimate of the experimental torsional strength.

## NOMENCLATURE

- $f'_c$  = Concrete compressive strength, psi or MPa.  
 $f_r$  = Modulus of rupture, psi or MPa.  
 $f'_{sp}$  = Splitting tensile strength, psi or MPa.  
 $f'_t$  = The tensile strength of concrete, psi or MPa.  
 $L$  = Center-to-center span in mm or in.  
 $L/Y$  = Span/depth ratio.  
 $T_e$  = Elastic failure torque, kN.m.  
 $T_{exp}$  = Experimental torsional strength, kN.m.  
 $T_{np}$  = Nominal torsional strength of plain concrete beam, kN.m.  
 $T_p$  = Plastic failure torque, kN.m.  
 $T_{th}$  = Theoretical torsional strength, kN.m.  
 $X, Y$  = The width and depth of the rectangular section, respectively, mm or in.  
 $Y/X$  = Depth/width (aspect) ratio.  
 $\alpha_c$  = St. Venant's coefficient which depends on  $Y/X$  and varies from 0.208 to 0.333.

- $\alpha_p$  =  $(0.5 - X/6Y)$ , plastic coefficient.  
 $\alpha_T$  = Tension crack inclination angle, degrees.  
 $\alpha_C$  = Compression crack inclination angle, degrees.  
 $\theta$  = Angle of twist, radians.

## INTRODUCTION

Structural members with span/depth ratio less than five and loaded on the compression face are classified by the ACI Code 318-89 [1] as deep beams. Common examples of deep beams can be found in transfer girders used in multistory buildings to provide column offsets, in walls of rectangular tanks, and in shear walls [2]. However, the ACI Code 318-89 [1] does not contain any design specifications for deep beams under torsion.

In recent years, use of high-strength concrete with compressive strength in excess of 41 MPa (6,000 psi) has gained wide acceptance and application in construction industry. The major advantages of its use are its lower unit weight for a given strength, reduced member dimensions and reinforcement requirements and hence a more economical construction cost [3]. These advantages encouraged builders in using concrete of higher strength, even before the various aspects of its behavior in structural members were fully understood. Because of a knowledge-gap in this area, ACI Committee 363 [4] encouraged extensive research work on various aspects of high-strength concrete behavior at both material and structural levels. Some investigators have actively responded to this call [5-7]; however, no research work appears to have been carried out on the torsional behavior of deep beams using high-strength concrete [4,8]. The objective of this investigation is to study the behavior of deep concrete beams subjected to torsion and to correlate the influence of high concrete strength and beam aspect ratios with the torsional capacity.

## THEORETICAL TORSIONAL STRENGTH

Three theories are presently available in the literature [9-12] to predict the torsional capacity of shallow members of plain normal-strength concrete, namely, the elastic theory, the plastic theory and the skew-bending theory. Recently, modifications to the skew-bending equation have been proposed to predict the torsional capacity of high-strength plain concrete shallow beams [7] and normal-strength plain concrete deep beams [13].

## Elastic Theory

The behavior of a plain concrete torsional member can be described by St. Venant's elastic theory [9]. The Torsional failure of a plain concrete member is assumed to occur when the maximum principal tensile stress  $\sigma_{\max}$  becomes equal to the tensile strength of concrete  $f'_t$ . The elastic failure torque,  $T_e$ , can be expressed as:

$$T_e = \alpha_e X^2 Y f'_t \quad (1)$$

where:

- X, Y = Shorter and longer sides of the rectangular section, respectively, mm or in.
- $\alpha_e$  = St. Venant's coefficient which depends on Y/X, and varies from 0.208 to 0.333.
- $f'_t$  = Tensile strength of concrete, MPa or psi. A reasonable value of  $0.42\sqrt{f'_c}$  has been suggested by Hsu [10], where  $f'_c$  is in MPa.

## Plastic Theory

In the plastic theory [11], failure is assumed to occur when the maximum principal tensile stress reaches the tensile strength of concrete  $f'_t$ . The plastic failure torque,  $T_p$ , is expressed as:

$$T_p = \alpha_p X^2 Y f'_t \quad (2)$$

Where:

- $\alpha_p$  =  $(0.5-X/6Y)$ , a plastic coefficient which depends on Y/X, and varies from 0.333 to 0.5.

## Skew-Bending Theory

The skew-bending theory [12] has been proposed to predict the torsional strength,  $T_{np}$ , as:

$$T_{np} = \frac{X^2 Y}{3} (0.85 f_r) \quad (3)$$

Where:

- $f_r$  = modulus of rupture of concrete, MPa or psi.

Hsu [10] developed the following empirical equation to predict the nominal

torsional strength of plain concrete beam in terms of the concrete compressive strength provided that  $X > 4$  inches.

$$T_{np} = 6 (X^2 + 10) Y \sqrt{f'_c} \quad (\text{psi Units}) \quad (4)$$

Where:

$f'_c$  = compressive strength of concrete, psi.

### Modified Skew-Bending Equation for High-Strength Concrete Shallow Beams

Bakhsh et al. [7] showed experimentally that a better prediction of the nominal torsional capacity of high-strength plain concrete shallow beam,  $T_{np}$ , can be obtained by using the splitting tensile strength of the concrete,  $f'_{sp}$ , in the skew-bending equation in lieu of  $0.85 f_c$ . Thus

$$T_{np} = \frac{X^2 Y}{3} f'_{sp} \quad (5)$$

Where:

$f'_{sp}$  = splitting tensile strength of concrete, MPa or psi.

### Modified Skew-Bending Equation for Normal-Strength Concrete Deep Beams

Akhtaruzzaman and Hasnat [13] showed that a better prediction of the nominal torsional strength of plain concrete deep beam,  $T_{np}$ , can be obtained by using  $f'_{sp}$  in Eq. (3) in lieu of  $f_c$ ,

$$T_{np} = \frac{X^2 Y}{3} (0.935 f'_{sp}) \quad \text{for } L/Y \geq 3.0 \quad (6)$$

$$T_{np} = \frac{X^2 Y}{3} f'_{sp} (1.34 - 0.08 L/Y) \quad \text{for } L/Y < 3.0 \quad (7)$$

Where:

$L$  = Center-to-center span, mm or in.

$L/Y$  = span/depth ratio.

## ACI Torsional Design Criteria

Although ACI Code 318-89 [1] does not have any design provision for deep beams under torsion, the Code does require that the nominal torsional strength of a plain concrete shallow member to be:

$$T_{np} = \frac{X^2 Y}{3} (0.2 \sqrt{f'_c}) \quad (S.I. \text{ Units}) \quad (8)$$

$$T_{np} = \frac{X^2 Y}{3} (2.4 \sqrt{f'_c}) \quad (\text{psi Units}) \quad (9)$$

## EXPERIMENTAL PROGRAM

A total of twenty high-strength plain concrete deep beams were tested under the action of pure torsion (Table 1). The beams were divided into four groups, each consisting of five specimens. The beams were designated by one letter and two numbers. The letter B designates a beam, the first number identifies the compressive strength group, while the second number identifies the depth/width (aspect) ratio. The major variables in this study were the concrete compressive strength and depth/width ratio. Four different concrete compressive strengths with values of 51.01 MPa (7,400 psi), 58.53 MPa (8,500 psi), 76.60 MPa (11,000 psi) and 83.66 MPa (12,131 psi) were used.

The depth/width ratio was varied from 1.0 to 5.0 with an increment of 1.0. All beams had a constant cross-sectional area of 40,000 mm<sup>2</sup> and a span/depth ratio of 4.0. The span length was varied to maintain a constant span/depth ratio.

Type I portland cement, sand with a fineness modulus of 2.8, and a crushed coarse aggregate of maximum size of 10 mm (3/8 in.) were used. Light gray silica fume having a specific gravity of about 2.2 (compared to 3.1 for ordinary portland cement) was used to increase concrete strength. The bulk density of silica fume was approximately 600 kg/m<sup>3</sup> (37.4 lb/ft<sup>3</sup>) compared to about 1200 kg/m<sup>3</sup> (75 lb/ft<sup>3</sup>) for ordinary portland cement. A superplasticizer was used to reduce the water requirement. This resulted in a lower W/C ratio which without affecting the workability, contributed to strength enhancement.

The concrete was placed in three layers in the formwork and was internally vibrated immediately after the placement of each layer. The control specimens comprised of 150x300 mm (6x12 in.) cylinders and 150x530 mm (6x6x12 in.)

Table 1: Dimensions of Deep Beams and Variables Involved in Test Program.

| Group No. | Beam No. | Span L (m) | X-Section Area X x Y (mm x mm) | L/Y | Y/X | $f'_c$ (MPa) |
|-----------|----------|------------|--------------------------------|-----|-----|--------------|
| 1         | B-11     | 0.8        | 200 x 200                      | 4   | 1   | 51.01        |
|           | B-12     | 1.2        | 135 x 296                      | 4   | 2   | 51.01        |
|           | B-13     | 1.4        | 114 x 350                      | 4   | 3   | 51.01        |
|           | B-14     | 1.6        | 100 x 400                      | 4   | 4   | 51.01        |
|           | B-15     | 1.8        | 89 x 450                       | 4   | 5   | 51.01        |
| 2         | B-21     | 0.8        | 200 x 200                      | 4   | 1   | 58.53        |
|           | B-22     | 1.2        | 135 x 296                      | 4   | 2   | 58.53        |
|           | B-23     | 1.4        | 114 x 350                      | 4   | 3   | 58.53        |
|           | B-24     | 1.6        | 100 x 400                      | 4   | 4   | 58.53        |
|           | B-25     | 1.8        | 89 x 450                       | 4   | 5   | 58.53        |
| 3         | B-31     | 0.8        | 200 x 200                      | 4   | 1   | 75.60        |
|           | B-32     | 1.2        | 135 x 296                      | 4   | 2   | 75.60        |
|           | B-33     | 1.4        | 114 x 350                      | 4   | 3   | 75.60        |
|           | B-34     | 1.6        | 100 x 400                      | 4   | 4   | 75.60        |
|           | B-35     | 1.8        | 89 x 450                       | 4   | 5   | 75.60        |
| 4         | B-41     | 0.8        | 200 x 200                      | 4   | 1   | 83.66        |
|           | B-42     | 1.2        | 135 x 296                      | 4   | 2   | 83.66        |
|           | B-43     | 1.4        | 114 x 350                      | 4   | 3   | 83.66        |
|           | B-44     | 1.6        | 100 x 400                      | 4   | 4   | 83.66        |
|           | B-45     | 1.8        | 89 x 450                       | 4   | 5   | 83.66        |

prisms. The average strengths were based on the strength of three control cylinders and prisms tested on the day of testing the beams. The specimens were covered with a polyethylene sheet until 24 hours before testing to prevent loss of moisture. All beams and control specimens were prepared and cured under the same environmental conditions. Details of the concrete mix proportions and their strength characteristics are shown in Table 2.

The beams were tested under the action of pure torsion. Special bearings at the supports insured that the test beam was free to twist at one end while the other end was held against torsional rotation as shown in Fig. 1. The load was applied in small increments up to failure. At the end of each load increment, the torsional

Table 2: Details of Concrete Mixes and Resultant Strengths.

| Group No. | Mix proportion by weight C:F.A:C.A* | W/C Ratio | Plasticizer % | Silica Fume % | Slump (mm) | Compres. Strength $f'_c$ (MPa)** | Spli.Tensile Strength $f'_{sp}$ (MPa)** | Modulus of Rupture $f_r$ (MPa)** |
|-----------|-------------------------------------|-----------|---------------|---------------|------------|----------------------------------|---|----------------------------------|
| 1         | 1:1.8:1.2                           | 0.37      | 1.5           | -             | 250        | 51.01                            | 4.47                                    | 6.14                             |
| 2         | 1:1.2:1.8                           | 0.27      | -             | -             | 60         | 58.53                            | 4.70                                    | 6.36                             |
| 3         | 1:1:2                               | 0.26      | 5.0           | 10            | 20         | 75.60                            | 6.03                                    | 10.23                            |
| 4         | 1:1:2                               | 0.23      | 5.0           | 10            | 33         | 83.66                            | 6.83                                    | 12.24                            |

\* C = Cement, F.A = Fine Aggregate, C.A = Coarse Aggregate.

\*\* Average value of three specimens.

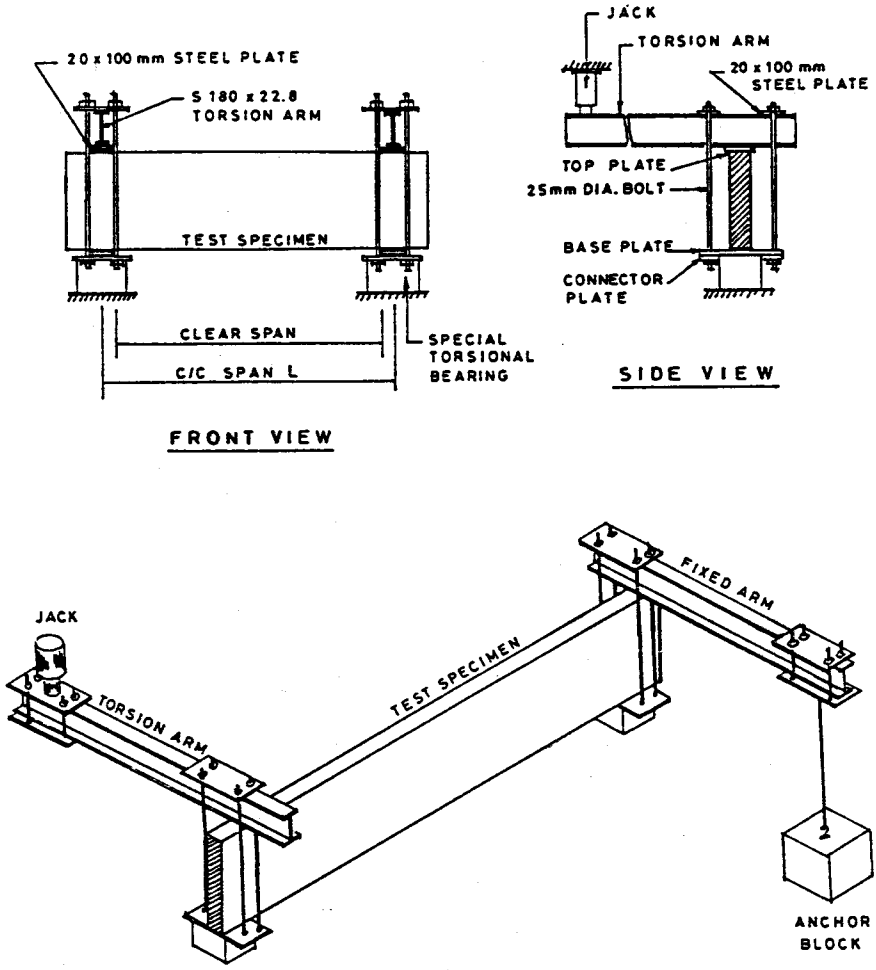


Figure 1: Testing set-up

rotations of the beam at its loaded end and at fixed end were recorded. Any crack development and propagation on the beam surfaces, were carefully followed and documented. The inclinations of failure cracks were measured at the end of a test.

### TEST RESULTS

The data obtained from testing sources were recorded and analyzed to study the effect of the depth/width ratio, the concrete strength, and the twist characteristics on the general behavior of the specimens. Orientation of crack formations were recorded and analyzed. Also, the experimental torsional strength



of the tested beams were compared with the theoretical values.

### Torque-Twist Relationship

Figure 2 shows the torque-twist relationship for the tested beams. The torque-twist curves are approximately linear upto 40 % of the respective torsional strengths; thereafter, the curves become nonlinear with reduced torsional stiffness.

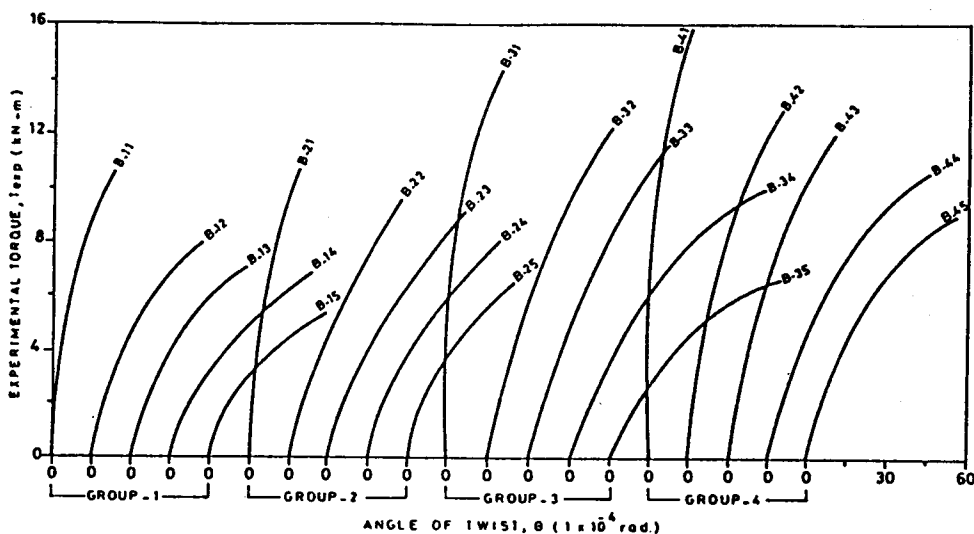


Figure 2: Torque - twisting angle relationship

For a given concrete compressive strength, the angle of twist ( $\Theta$ ) increases with an increase of Y/X ratio as shown in Fig. 2. This indicates that the energy absorbed (area under the T- $\Theta$  curves) increases with the increase of Y/X ratio. The angle of twist ( $\Theta$ ) decreases (i.e., stiffness increases) with the increase of concrete compressive strength.

### Crack Pattern on Vertical Side

During the test, no surface cracks were observed on any of the test beams. On reaching the failure loads, the beams failed suddenly and violently along inclined surfaces. Fig. 3 shows some typical crack patterns. The inclinations of failure-cracks for the two vertical faces of the tested beams are presented in Table 3. These inclinations were different in the two opposite vertical sides and depended on the depth/width ratio and the concrete compressive strength. The effects of depth/width ratio on the crack- inclination angle for the tension and compression cracks are shown in Figs. 4 and 5.

Table 3: Inclination of Failure Crack with Beam Axis for the Tested Beams.

| Depth/Width<br>(Y/X)<br>Ratio | Inclination of Tension<br>Crack (deg.) |                                    |                                    |                                    | Inclination of Compression<br>Crack (deg.) |                                    |                                    |                                    |
|-------------------------------|--|------------------------------------|------------------------------------|------------------------------------|--|------------------------------------|------------------------------------|------------------------------------|
|                               | Group # 1<br>$f'_c=50.01$<br>(MPa)     | Group # 2<br>$f'_c=58.53$<br>(MPa) | Group # 3<br>$f'_c=75.60$<br>(MPa) | Group # 4<br>$f'_c=83.66$<br>(MPa) | Group # 1<br>$f'_c=50.01$<br>(MPa)         | Group # 2<br>$f'_c=58.53$<br>(MPa) | Group # 3<br>$f'_c=75.60$<br>(MPa) | Group # 4<br>$f'_c=83.66$<br>(MPa) |
| 1                             | 45.58                                  | 35.20                              | 44.57                              | 69.26                              | 27.04                                      | 40.79                              | 29.75                              | 61.43                              |
| 2                             | 46.56                                  | 48.86                              | 49.60                              | 56.83                              | 29.47                                      | 36.73                              | 36.87                              | 53.03                              |
| 3                             | 55.15                                  | 43.87                              | 53.80                              | 50.42                              | 42.54                                      | 33.73                              | 44.33                              | 49.40                              |
| 4                             | 47.84                                  | 45.88                              | 46.32                              | 51.85                              | 43.39                                      | 37.52                              | 40.63                              | 45.28                              |
| 5                             | 51.51                                  | 52.14                              | 58.23                              | 43.46                              | 46.78                                      | 49.70                              | 48.95                              | 49.51                              |

Effect of Aspect Ratio on Plain Concrete Deep Beams



Figure 3: Typical crack patterns

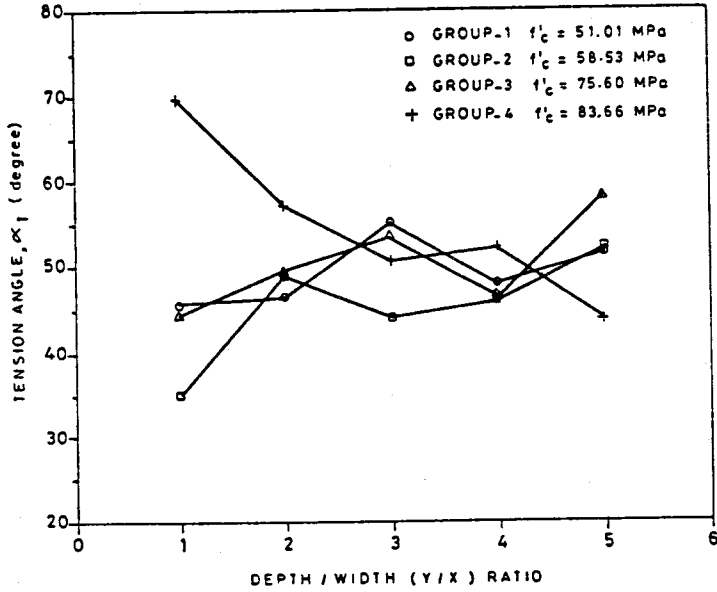


Figure 4: Effect of depth/width (Y/X) ratio on tension crack inclination

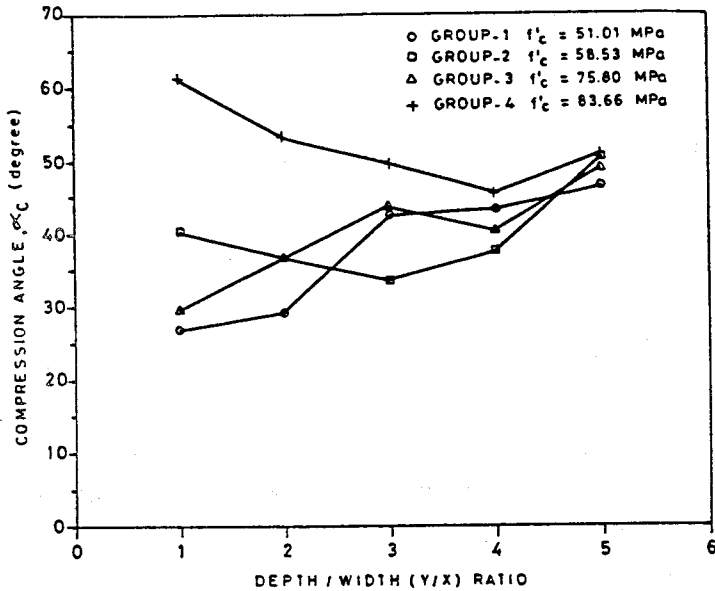


Figure 5: Effect of depth/width (Y/X) ratio on compression crack inclination

The inclinations of tension cracks of beams with high-strength concrete varied approximately from 35 to 69 degrees. This indicates that probably the skew-bending theory [10] which was based on a 45° failure plane needs to be modified. The inclination of compression crack was found to be always smaller than the corresponding tension crack, and varied from 27 to 61 degrees depending upon the depth/width ratio and the concrete compressive strength.

### Experimental Torsional Strength

The effect of the aspect ( $Y/X$ ) ratio on the experimental torsional strength ( $T_{exp}$ ) of the test beams are listed in Table 4 and plotted in Fig. 6. Decrease of the depth/width ( $Y/X$ ) ratio from 5 to 1 resulted in nonlinear increases in the torsional strength from 5.48 to 16.61 kN-m, depending on the concrete compressive strength.

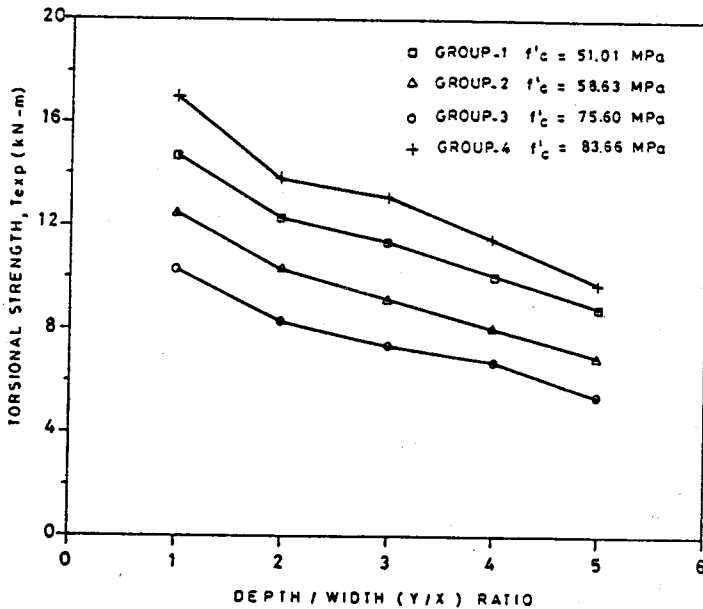


Figure 6: Effect of depth/width ( $Y/X$ ) ratio on the experimental torsional strength for tested beams

The torsional strengths of the tested beams increase with the increase of the concrete compressive strength for the same  $Y/X$  ratio as shown in Table 4 and Fig. 7. Test results showed that by increasing the concrete compressive strength from 51.01 to 83.66 MPa (7,400 to 12,131 psi) a rise in torsional strength between 17 to 76 % was observed for various  $Y/X$  ratios.

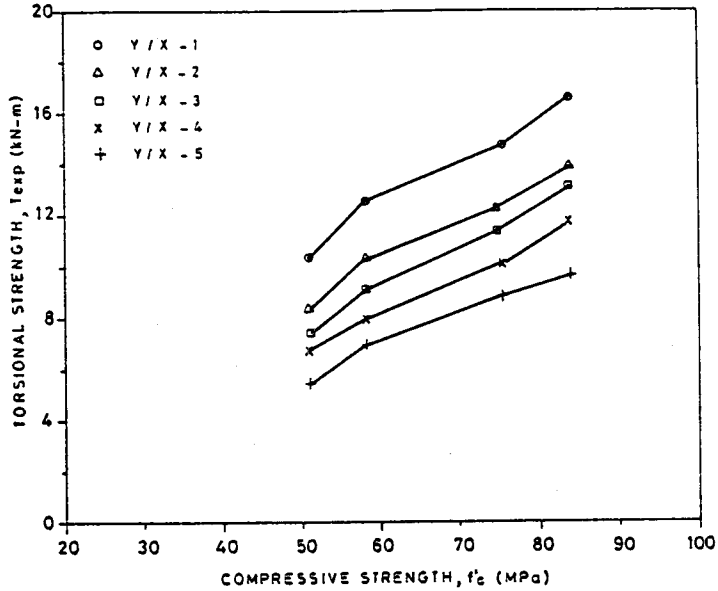


Figure 7: Effect of concrete compressive strength,  $f'_c$  on experimental torsional strength for tested beams

### Theoretical Torsional Strength

The theoretical torsional strength of tested beams had been estimated using the following methods:

1. Elastic theory (Eq. 1) .
2. Plastic theory (Eq. 2) .
3. Skew-bending theory in terms of the modulus of rupture (Eq. 3).
4. Skew-bending theory in terms of the concrete compressive strength (Eq.4).
5. Skew-bending theory in terms of the splitting tensile strength (Eq. 5).
6. Akhtaruzzaman and Hasnat equation (Eq. 6).
7. ACI Code equation for shallow beam (Eq. 8).

The experimental torsional strength of the tested beams and the corresponding theoretical torsional strength have been listed in Table 4 and plotted in Figs. 8 to 11. The elastic theory, plastic theory, skew-bending theory in terms of compressive strength, the equation proposed by Akhtaruzzaman and Hasnat and

Table 4: Experimental and Theoretical Torsional Strength for the Tested Beams.

| Group No. | Beam No. | Span L | Y/X | $f'_c$ MPa | Theoretical Torsional Strength Using |       |       |       |       |       |       |        | Experimental Torque kN-m | * ** ***                 |                          |                          |
|-----------|----------|--------|-----|------------|--------------------------------------|-------|-------|-------|-------|-------|-------|--------|--------------------------|--------------------------|--------------------------|--------------------------|
|           |          |        |     |            | Eq. 1                                | Eq. 2 | Eq. 3 | Eq. 4 | Eq. 5 | Eq. 6 | Eq. 8 | Eq. 11 |                          | $\frac{T_{exp}}{T_{th}}$ | $\frac{T_{exp}}{T_{th}}$ | $\frac{T_{exp}}{T_{th}}$ |
|           |          |        |     |            | kN.m                                 | kN.m  | kN.m  | kN.m  | kN.m  | kN.m  | kN.m  | kN.m   |                          |                          |                          |                          |
| 1         | B-11     | 0.8    | 1   | 51.01      | 4.99                                 | 7.99  | 13.92 | 7.49  | 11.92 | 11.15 | 3.80  | 12.92  | 10.46                    | 0.88                     | 0.81                     | 2.75                     |
|           | B-12     | 1.2    | 2   | 51.01      | 3.98                                 | 6.86  | 9.38  | 5.88  | 8.04  | 7.52  | 2.56  | 8.70   | 8.38                     | 1.04                     | 0.96                     | 3.27                     |
|           | B-13     | 1.4    | 3   | 51.01      | 3.64                                 | 6.09  | 7.91  | 5.49  | 6.78  | 6.34  | 2.16  | 7.34   | 7.43                     | 1.10                     | 1.01                     | 3.44                     |
|           | B-14     | 1.6    | 4   | 51.01      | 3.44                                 | 5.49  | 6.96  | 5.31  | 5.96  | 5.57  | 1.90  | 6.46   | 6.89                     | 1.16                     | 1.07                     | 3.63                     |
|           | B-15     | 1.8    | 5   | 51.01      | 3.10                                 | 5.00  | 6.20  | 5.21  | 5.31  | 4.96  | 1.69  | 5.75   | 5.48                     | 1.03                     | 0.95                     | 3.24                     |
| 2         | B-21     | 0.8    | 1   | 58.53      | 5.35                                 | 8.56  | 14.42 | 7.84  | 12.53 | 11.72 | 4.07  | 13.84  | 12.62                    | 1.01                     | 0.91                     | 3.10                     |
|           | B-22     | 1.2    | 2   | 58.53      | 4.26                                 | 7.35  | 9.72  | 6.16  | 8.45  | 7.90  | 2.74  | 9.32   | 10.36                    | 1.23                     | 1.11                     | 3.78                     |
|           | B-23     | 1.4    | 3   | 58.53      | 3.90                                 | 6.52  | 8.20  | 5.74  | 7.13  | 6.66  | 2.31  | 7.85   | 9.17                     | 1.29                     | 1.17                     | 3.97                     |
|           | B-24     | 1.6    | 4   | 58.53      | 3.63                                 | 5.89  | 7.21  | 5.55  | 6.27  | 5.86  | 2.03  | 6.90   | 8.05                     | 1.28                     | 1.17                     | 3.97                     |
|           | B-25     | 1.8    | 5   | 58.53      | 3.32                                 | 5.35  | 6.42  | 5.46  | 5.58  | 5.22  | 1.81  | 6.15   | 6.94                     | 1.24                     | 1.13                     | 3.83                     |
| 3         | B-31     | 0.8    | 1   | 75.60      | 6.08                                 | 9.73  | 23.19 | 8.53  | 16.59 | 15.04 | 4.62  | 15.71  | 14.79                    | 0.89                     | 0.94                     | 3.20                     |
|           | B-32     | 1.2    | 2   | 75.60      | 4.85                                 | 8.35  | 15.64 | 6.70  | 11.18 | 10.14 | 3.12  | 10.61  | 12.36                    | 1.11                     | 1.17                     | 3.96                     |
|           | B-33     | 1.4    | 3   | 75.60      | 4.45                                 | 7.41  | 13.18 | 6.26  | 9.43  | 8.55  | 2.63  | 8.94   | 11.45                    | 1.21                     | 1.28                     | 4.35                     |
|           | B-34     | 1.6    | 4   | 75.60      | 4.19                                 | 6.69  | 11.59 | 6.05  | 8.29  | 7.52  | 2.31  | 7.85   | 10.14                    | 1.22                     | 1.29                     | 4.39                     |
|           | B-35     | 1.8    | 5   | 75.60      | 3.77                                 | 6.08  | 10.33 | 5.94  | 7.39  | 6.70  | 2.06  | 7.00   | 8.86                     | 1.20                     | 1.27                     | 4.30                     |
| 4         | B-41     | 0.8    | 1   | 83.66      | 6.30                                 | 10.23 | 27.74 | 8.69  | 18.21 | 17.03 | 4.88  | 16.59  | 16.61                    | 0.91                     | 1.00                     | 3.40                     |
|           | B-42     | 1.2    | 2   | 83.66      | 5.29                                 | 8.79  | 18.71 | 6.80  | 12.28 | 11.48 | 3.29  | 11.19  | 13.79                    | 1.12                     | 1.23                     | 4.19                     |
|           | B-43     | 1.4    | 3   | 83.66      | 4.63                                 | 7.79  | 15.78 | 6.33  | 10.36 | 9.68  | 2.77  | 9.42   | 12.93                    | 1.25                     | 1.37                     | 4.67                     |
|           | B-44     | 1.6    | 4   | 83.66      | 4.41                                 | 7.05  | 13.87 | 6.10  | 9.11  | 8.52  | 2.44  | 8.30   | 11.57                    | 1.27                     | 1.39                     | 4.74                     |
|           | B-45     | 1.8    | 5   | 83.66      | 4.04                                 | 6.40  | 12.36 | 5.99  | 8.12  | 7.59  | 2.17  | 7.39   | 9.63                     | 1.19                     | 1.30                     | 4.44                     |

\* Value given by Eq. 5, \*\* Value given by Eq. 11, \*\*\* Value given by Eq. 8.

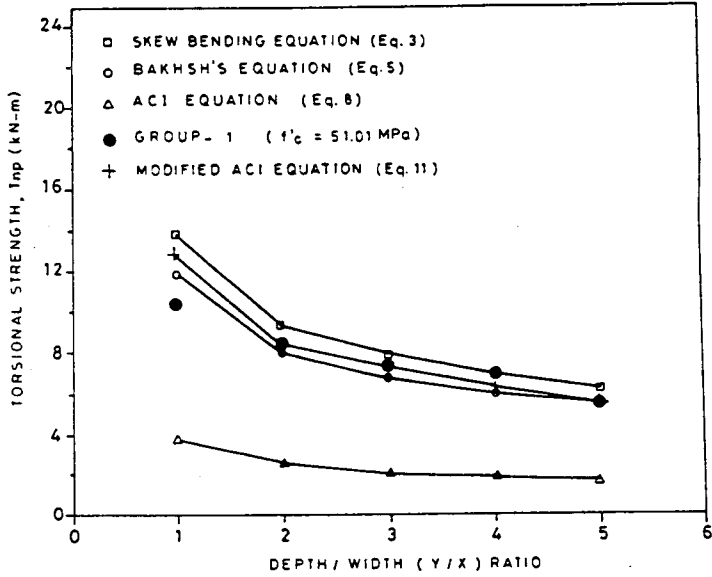


Figure 8: Effect of depth/width (Y/X) ratio on the experimental and theoretical torsional strength for tested beams of group-1

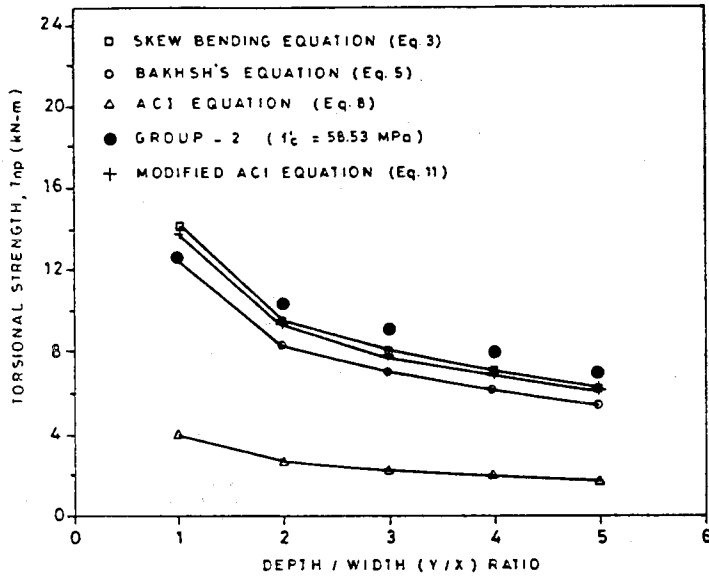


Figure 9: Effect of depth/width (Y/X) ratio on the experimental and theoretical torsional strength for tested beams of group-2



Effect of Aspect Ratio on Plain Concrete Deep Beams

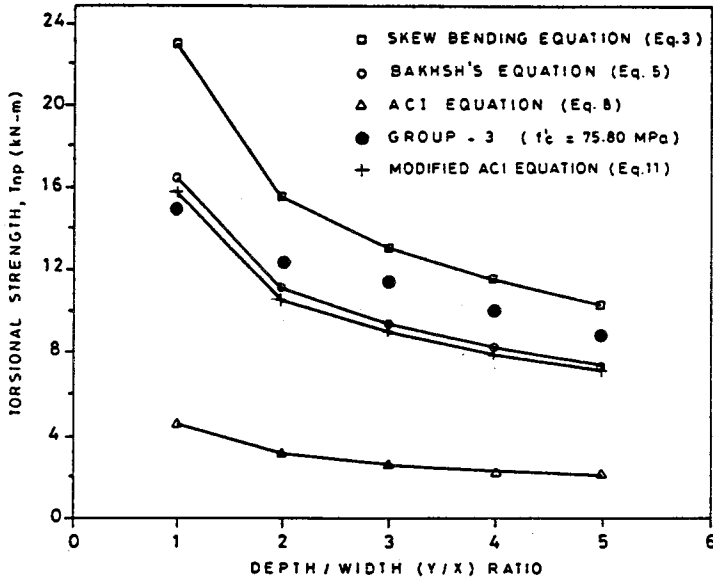


Figure 10: Effect of depth/width (Y/X) ratio on the experimental and theoretical torsional strength for tested beams of group-3

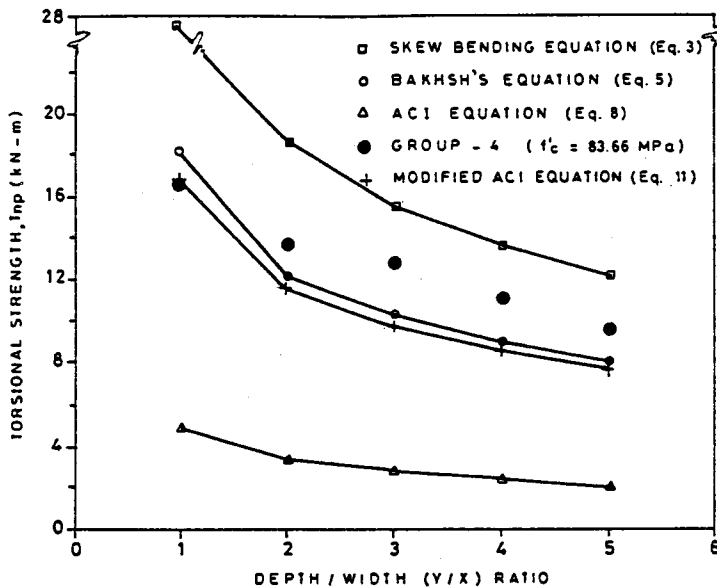


Figure 11: Effect of depth/width (Y/X) ratio on the experimental and theoretical torsional strength for tested beams of group-4

the ACI Code 318-89 equation always under-estimated the torsional strength of the tested beams by 77 to 179 %, 10 to 66 %, 5 to 104 %, 8 to 38 %, and 175 to 374 %, respectively. The skew-bending theory in terms of modulus of rupture over-estimated the torsional capacity of the tested beams of the first, third and fourth groups by 1 to 33 %, 14 to 57 %, and 20 to 67 %, respectively, and under-estimated the torsional strength for the beams of the second group in the region of  $Y/X > 2.0$  by 7 to 13 %. The theoretical torsional strength computed in terms of the splitting tensile strength (Eq. 5) gave good prediction for the experimental torsional strength and can be taken as a lower-bound approach for the tested high-strength concrete deep beams.

A comparison between the skew-bending theory (Eq. 3) and the ACI Code (Eq. 8) indicates that the ACI Code has taken the term  $0.85 f_r$  conservatively as  $0.2 \sqrt{f'_c}$ . However, based on a regression analysis of thirteen high-strength concrete mix proportion results, Bakhsh et al [7] showed experimentally that a linear relationship is existed between the modulus of rupture and the square root of the concrete compressive strength as:

$$f_r = 0.8 \sqrt{f'_c} \quad (S.I. Units) \quad (10)$$

Therefore, a better prediction of the nominal torsional capacity of high-strength plain concrete deep beams,  $T_{np}$ , can be obtained by using  $0.85 f_r$  ( $0.85$  Eq.10), in the ACI Code 318-89 equation (Eq. 8) in lieu of  $0.2 \sqrt{f'_c}$ , thus

$$T_{np} = \frac{X^2 Y}{3} (0.68 \sqrt{f'_c}) \quad (S.I. Units) \quad (11)$$

Table 4 and Figs. 8 through 11 show the experimental torsional strength and the theoretical torsional strength computed on the basis of the modified equation (Eq.11). The proposed equation gives  $T_{exp}/T_{th}$  ratio ranging from 0.81 to 1.39 as compared to 2.75 to 4.74 if the ACI Code 318-89 equation (Eq. 8) is used.

## CONCLUSIONS

Based on the test results of twenty high-strength plain concrete deep beams under torsion, the following conclusions were drawn:

1. The angle of twist of high-strength plain concrete deep beams increases with the increase of aspect ( $Y/X$ ) ratio and with the decrease of the compressive strength.

2. All test beams were observed to fail suddenly and violently (brittle failure).
3. The torsional capacity of high-strength plain concrete deep beams increases as the concrete compressive strength increases and the depth/width ratio decreases.
4. The design equation for torsion of ACI Code (318-89) appears to be highly conservative in predicting the torsional strength of the tested beams by 175 to 374 %.
5. The ACI Code 318-89 design torsional equation for normal-strength concrete shallow beams was modified to predict the torsional capacity of high-strength plain concrete deep beams as follows:

$$T_{np} = \frac{X^2 Y}{3} (0.68\sqrt{f'_c}) \quad (S.I. \text{ Units})$$

6. The skew-bending theory based on splitting tensile strength gave good estimate of the experimental torsional strength and can be taken as a lower-bound approach.

## REFERENCES

1. **ACI Committee 318, 1989**, Building Code Requirements for Reinforced Concrete (318-89), American Concrete Institute, Detroit, Michigan, pp. 353.
2. **Nilson, A.H., and Winter, G., 1991**, Design of Concrete Structure, 11th Edition, McGraw-Hill Book Company, New York, pp. 904.
3. **Burge, A.T., Sept. 1983**, 14,000 psi in 24 Hours, Concrete International, Vol. 5, No. 9, pp. 36-41.
4. **ACI Committee 363, 1987**, Research Needs for High-Strength Concrete (ACI 363-IR-87), ACI Materials Journal, Proceedings Vol. 84, No. 6, Nov. - Dec., pp. 559-561.
5. **Castillio, C., and Durani, A.J., 1990**, Effect of Transient High Temperature on High-Strength Concrete, ACI Materials Journal, Proceedings Vol. 87, No. 1, Jan. - Feb., pp. 47-53.

6. **Roller, J., and Russel, G., 1990**, Shear Strength of High-Strength Concrete Beams with Web Reinforcement, *ACI Structural Journal, Proceedings* Vol. 87, No. 2, March - April, pp. 191-198.
7. **Bakhsh, H., Wafa, F.F., and Akhtaruzzaman, A., 1990**, Torsional Behavior of Plain High-Strength Concrete Beams, *ACI Structural Journal, Proceedings* Vol. 87, No. 5, Sept. - Oct., pp. 587-588.
8. **ACI Committee 363, 1984**, State-of-the-Art Report on High-Strength Concrete, *ACI Journal, Proceedings* Vol. 81, No. 4, July - Aug., pp. 365-387.
9. **Nawy, G.E., 1985**, Reinforced Concrete, Prentice-Hall Inc., Englewood Cliffs, New Jersey, pp. 227.
10. **Hsu, T.T.C., 1984**, Torsional Reinforced Concrete, Van Nostrand Reinhold Company, New York, pp. 516.
11. **Hsu, T.T.C., 1968**, Torsion of Structural Concrete-Plain Rectangular Sections, *Torsion of Structural Concrete, SP-18*, American Concrete Institute, Detroit, pp. 203-238.
12. **ACI Committee 438, 1969**, Tentative Recommendations for the Design of Reinforced Concrete Members to Resist Torsion, *ACI Journal, Proceedings* Vol. 66, No. 1, January, pp. 576-588.
13. **Akhtaruzzaman, A.A., and Hasnat, A., Jan. - Feb. 1989**, "Torsion in Deep Beams with an Opening," *ACI Structural Journal, Proceedings* Vol. 86, No. 1, pp. 20-25.